Adaptive Path Planning for Multi-Agent Systems Using Improved Artificial Potential Field with Neural Network Approximation

Zhipeng Zhu, Zhao Zhang, Hongyan Zhou, and Xue-Bo Chen

Abstract—**This paper studies obstacle and collision avoidance strategies for nonlinear second-order multi-agent systems (MAS) formation control. Due to the uncertainties and complexities in nonlinear systems, including external disturbances and communication delays, radial basis function (RBF) neural network control is employed to address the control requirements of nonlinear terms in the system. In addition, as traditional artificial potential fields (APF) based obstacle avoidance algorithms have limitations, this paper applies an improved APF algorithm for collision avoidance and obstacle avoidance in multi-agent systems formation control. The stability and feasibility of the proposed approach are proved based on the Lyapunov stability theory. Simulation experiments further validate the effectiveness of the formation control strategy.**

Index Terms—**multi-agent systems, formation control, obstacle avoidance, collision avoidance, neural network, artificial potential field.**

I. Introduction

In recent years, multi-agent systems (MAS) have garnered substantial attention within the academic community. Researchers have conducted comprehensive investigations into various facets of MAS, encompassing consensus control [1, 2], flocking control [3], and formation control [4, 5]. Formation control, in particular, has found extensive applications in both industrial and military contexts, including scenarios like underwater swarm exploration and aerial swarm reconnaissance. Consequently, formation control has become an indispensable component of MAS research. We utilize several methodologies employed for formation control, such as the leader-follower method [6, 7], virtual structure method [8, 9], and behavior-based method [10]. Typically, the leader-follower method is applied in engineering practice, owing to its innate capacity to effectively synchronize information among individual agents, coupled with graph theory. As technology advances, formation control systems' demands and performance expectations have gradually escalated. Scholars have embarked on research encompassing various system types, spanning linear [11] and nonlinear [12], high-order [13], heterogeneous [14], and non-affine [15] systems. In terms of performance requirements, researchers have conducted studies on event-triggered control [16], observer-based control [17], predictive performance control [18].

In practical applications, Nonlinear dynamic systems often model MASs. For instance, Y. Guo et al. [19] investigated nonlinear second-order systems in the presence of external disturbances. They addressed high-order nonlinear system tracking control using the back-stepping method [20]. The system equations can also be complex and unknown. G. WEN et al. [21] proposed an adaptive neural network control approach to address this challenge. This approach utilizes neural networks to approximate the unknown system dynamics, enabling adaptive control with automatic adjustments of control parameters to accommodate system changes.

Moreover, it is essential to consider real-world conditions where external disturbances and time delays are prevalent. Literature [22] accounts for external disturbances that MAS may encounter during formation control. It applies neural networks and adaptive dynamic sliding mode control techniques to estimate and compensate for these external disturbances, thus enhancing system robustness. The study in [16] looks at the impact of input time delays on system performance and introduces a delay-dependent strategy to ensure control stability and performance. This method is validated through theoretical analysis and numerical simulations for its effectiveness and robustness. This research actively addresses practical challenges in MAS, like delays and communication overhead, offering theoretical insights and practical solutions.

Research on obstacle avoidance is a fundamental aspect of MAS formation control. Scholars have introduced a variety of techniques for path planning, such as online optimal control techniques [23, 24], model predictive control methods [25, 26], reinforcement learning [27, 28], and intelligent algorithms [29]. Among these methods, the APF method has been widely adopted in the MAS literature [30–33] due to its simplicity and underlying principles. Q. Shi et al. [32] proposed an adaptive leader-follower formation control method. In this approach, follower agents maintain formation and avoid collisions with other agents, primarily employing the APF method. Similarly, the APF method was used to achieve formation control while simultaneously avoiding collisions with both agents and obstacles [33]. However, the traditional APF method has certain algorithmic shortcomings that can result in the system getting trapped in local minima under specific circumstances. Although the methods to address this

Manuscript received August 27, 2023; revised December 24, 2023. The research work was supported by the National Natural Science Foundation of China (71571091 and 71771112), the State Key Laboratory of Synthetical Automation for Process Industries (PAL-N201801), and the Excellent Talent Training Project of University of Science and Technology Liaoning (2019RC05).

Zhipeng Zhu is a postgraduate student of School of Computer Science and Software Engineering, University of Science and Technology Liaoning, Anshan, 114051, China. (e-mail: 15962093666@163.com).

Zhao Zhang is an associate professor of School of Computer Science and Software Engineering, University of Science and Technology Liaoning, Anshan, 114051, China. (corresponding author, e-mail: zhangzhao333@hotmail.com).

Hongyan Zhou is a doctoral student of School of Electronic and Information Engineering, University of Science and Technology Liaoning, Anshan, 114051, China. (e-mail: zhou321yan@163.com).

Xue-Bo Chen is a professor of School of Electronic and Information Engineering, University of Science and Technology Liaoning, Anshan, 114051, China. (e-mail: xuebochen@126.com).

local minimum problem were introduced in [30, 31], these primarily focused on enhancing the gravitational field. It is crucial to note that many of these methods originate from a single-agent context, and most of the existing MAS literature does not address this issue. Furthermore, in most literature, obstacles and agents are treated as point-like entities. Nevertheless, in practical, real-world applications, each obstacle and agent represent a rigid body with a distinct shape. This paper introduces an enhanced APF formula based on S. Yang et al. [33], improved real-world application obstacle avoidance and collision avoidance capabilities. It is worth noting that the concept of normal force has been introduced to address the issue of getting stuck in local minima.

Built upon the aforementioned discussion, this paper's contributions can be summarized as follows:

1) Different from linear systems [11], the system adopted in this paper is a second-order nonlinear system with unknown nonlinear terms and external disturbances with time delays, which better describes real-world engineering MAS.
2) The adaptive control used in this paper is based on RBFNN, which has different adaptability than traditional adaptive control. It can better approximate unknown nonlinear terms and adapt to more system scenarios. In addition, it requires fewer parameters and reduces computational complexity compared to C. L. P. Chen et al. [20].
3) This study employs an improved APF method, which differs from traditional approaches in that the obstacle and agent are not seen as a point, different distances are set in this paper, it can address the issue of local minimum traps in specific situations, thereby enhancing the robustness of the overall obstacle avoidance requirements.

This paper is structured as follows. Preliminary work and modeling are in Section II, controller design and stability analysis of the system are in Section III, Section IV is devoted to the demonstration of the results of the experimental approach using simulation examples, and Section V is devoted to the conclusions obtained and the outlook for future work.

II. Preliminaries and modeling

A. System modelling

A system model consisting of nonlinear equations was chosen to describe the overall state of the actual system, and a disturbance equation and a communication time delay were added to the nonlinear equations. In a MAS, the generalized second-order nonlinear equation for each agent i is as follows:

$$\begin{aligned} \dot{p}_i &= v_i \\ \dot{v}_i &= f_i(p_i, v_i, t-\tau) + \delta_i(t) + g_i(p_i, v_i, t-\tau)u_i \end{aligned} \tag{1}$$

where $p_i = [p_{i1}, p_{i2}, \cdots, p_{im}]^\top \in \mathbb{R}^m$, $v_i = [v_{i1}, v_{i2}, \cdots, v_{im}]^\top \in \mathbb{R}^m$ denote the vectors of position and velocity of agents, respectively. $f_i(p_i, v_i, t-\tau) = [f_i(p_{i1}, v_{i1}, t-\tau), \cdots, f_{1m}(p_{1m}, v_{1m}, t-\tau)]^\top \in \mathbb{R}^m \to \mathbb{R}^{m\times m}$ is a smooth unknown nonlinear equation with communication time delay, $g_i(p_i, v_i, t-\tau) = [g_{i1}(p_{i1}, v_{i1}, t-\tau), \cdots, g_{im}(p_{im}, v_{im}, t-\tau)]^\top \in \mathbb{R}^m \to \mathbb{R}^{m\times m}$ is an nonlinear gain matrix, where τ is time delay. $\delta_i(t) = [\delta_{i1}(t), \cdots, \delta_{im}(t)]^\top$ denotes the external disturbances from the external environment. $u_i(t) = [u_{i1}(t), \cdots, u_{im}(t)]^\top$ is an input to the follower agent of each.

In addition, the leader is the agent that leads the movement of the follower, and its dynamics equation is as follows:

$$\begin{aligned} \dot{p}_l &= v_l \\ \dot{v}_l &= f_l(p_l, v_l) + u_l \end{aligned} \tag{2}$$

where $p_l = [p_{l1}, p_{l2}, \cdots, p_{lm}]^\top \in \mathbb{R}^m$, $v_l = [v_{l1}, v_{l2}, \cdots, v_{lm}]^\top \in \mathbb{R}^m$ are the leader's position and velocity vectors, respectively, $u_l = [u_{l1}, \cdots, u_{lm}]^\top \in \mathbb{R}^m$ is the controller input to the leader. in which $f_l(p_l, v_l) = [f_{l1}(p_{l1}, v_{l1}), \cdots, f_{lm}(p_{lm}, v_{lm})]^\top \in \mathbb{R}^m$ is a known function.

Define the position and velocity tracking error variables of agent i as follows [34]:

$$\begin{aligned} e_i^p &= p_i - p_l - \Xi_i \\ e_i^v &= v_i - v_l \end{aligned} \tag{3}$$

where e_i^p, e_i^v is a vector representing the desired relative position between agent i and leader, i.e., the shape of the formation.

Definition 1 ([35]). *In a multi-agent system, the formation goal is completed when e_i^p and e_i^v equal to zero as time tends to infinity, i.e.* $\lim_{t\to\infty} \|e_i^p\| = 0$, $\lim_{t\to\infty} \|e_i^v\| = 0$.

The control objective: In the MAS, each agent follows a leader agent in a particular formation for trajectory tracking, as the system is nonlinear and has external disturbances and time delays. In addition, each agent cannot collide with each other, and the agent cannot collide with fixed obstacles in the environment, so in summary, the controller is required to have the following requirements:

1) Each agent can move consistently according to a certain formation.
2) Agents can adaptively complete control to cope with unknown factors in the environment.
3) Agents can complete obstacle avoidance and collision avoidance.

Assumption 1 ([36]). *The nonlinear function $g_i(\cdot) \in \mathbb{R}^m$ is either a negative or positive definite symmetric matrix. Its eigenvalues $\lambda_1(g_i(\cdot)), \cdots, \lambda_m(g_i(\cdot))$ satisfy that $0 < \underline{g_i} \le \|\lambda_1(g_i(\cdot))\|, \cdots, \|\lambda_m(g_i(\cdot))\| < \infty, i = 1, \cdots, n$, where $\underline{g_i}$ are a constant. Without loss of generality, we further assume $\lambda_1(g_i(\cdot)), \cdots, \lambda_m(g_i(\cdot)) > \underline{g_i} > 0, i = 1, \cdots, n$.*

Assumption 2 ([37]). *The function $f_l(\cdot) \in \mathbb{R}^m$ is bounded, and there exist a positive constant α which satisfy $\|f_l(\cdot)\| < \alpha$, $\forall t \in \mathbb{R}^+$,*

Assumption 3 ([33]). *The velocity states of agents v_l and v_i are not equal to zero and are also bounded.*

Remark 1. *According to the leader-follower theory, the leader and follower are two different types of agents. The leader is responsible for leading the follower for the overall movement, so in reality, the dynamics equations of the leader need not be too complicated.*

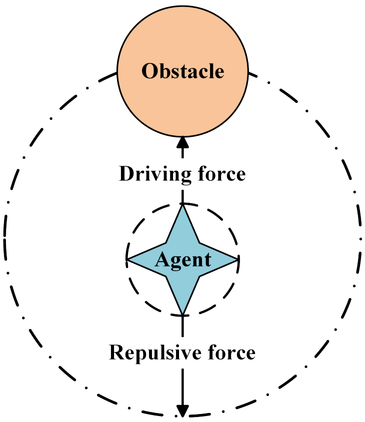

(a) One obstacle

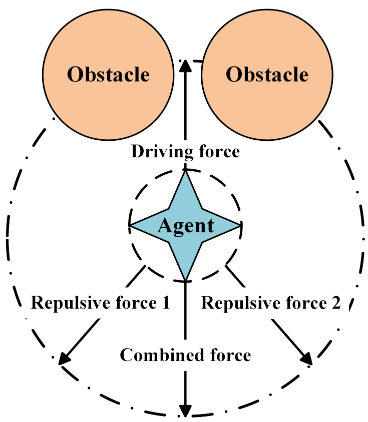

(b) Multiple obstacles

Fig. 1: Two cases of falling into local minima

B. Algebraic graph theory

In MAS, it is common to use graph theory to describe the communication relationships between agents. In this paper, a weighted directed graph $G = (V, E, A)$ is used to denote a MAS, where $V = \{v_1, v_2, ...v_n\}$ is the node-set, $E = \{e_1, e_2, ..., e_m\}$ is the edge between agents and $A = [a_{ij}]$ is the weighted adjacency matrix. The set of neighbor $N_i = \{v_j \mid v_j \in V, e_{ij} \in E\}$ denotes the set of all agents that have information exchange with agent v_i.The Laplacian matrix of digraph G is defined as:

$$L = D - A \tag{4}$$

where $D = diag(\sum_{j=1}^{n} a_{ij}, i = 1, ..., n)$.

We define the leader adjacency weight matrix $B = diag(b_1, b_2, ..., b_n)$, of which b_i denotes the connection between the leader and agents. Typically, we assume that at least one agent is connected to the leader. Therefore, $b_1 + b_2 + ... + b_n > 0$.

C. Radial basis neural networks and approximation of nonlinear functions

Radial basis neural network control (RBFNNC) is commonly used to approximate nonlinear terms in a controller. This paper uses RBFNN to approximate unknown nonlinear equations with external disturbance and communication time delays to achieve adaptive control. RBFNN approximates the continuous equation $\phi(z) : \mathbb{R}^n \to \mathbb{R}^m$ in the following form:

$$\phi(z) = W^\top H_i(z_i) \tag{5}$$

where $W \in \mathbb{R}^{\eta \times m}$ is the weight of the kernel function, $H_i(z_i) = [h_1(z), \cdots, h_\eta(z)]^\top$ is the artificially chosen kernel function, where η denotes the number of neurons, and the kernel function we normally use is a Gaussian function, which takes the following form:

$$h_j(z) = exp(\frac{\|z - \mu_j\|}{2K_N^2}), j = 1, \cdots, \eta \tag{6}$$

where μ_j is the central vector of the Gaussian function, which is contained in each hidden layer node.
The normal form of the function after approximation by the neural network is as follows:

$$\Phi = W^{*\top} H_i(z_i) + \epsilon_i(z_i) \tag{7}$$

where W^* is the adaptive law $\dot{\hat{W}}$ obtained by Lyapunov stability analysis, after constantly updating the weights to the optimal weights, $\epsilon_i(z_i) \in \mathbb{R}^m$ is an approximate error, the mathematical form of W^* is as follows:

$$W^* = arg \min_{W \in \Omega} [sup|\hat{\phi} - \Phi|] \tag{8}$$

D. Improved artificial potential field

Like much of the literature, the traditional APF method is used to accomplish obstacle avoidance for MAS in papers [32] and [33]. They both ignore the fact that the traditional APF method has the algorithmic disadvantage of being prone to fall into local minima, as shown in Figure 1(a) and 1(b). When the agent is in the same line as the obstacle and the forward direction, the agent will stop moving or moving in the opposite direction, i.e., fall into a local minima trap. We need to design a solution to cope with this problem.

For the local minima problem, this paper adopts the method that the normal force escapes from the local minima. First, the definition of falling into a local minima trap is given as follows:

Definition 2. *If the directional angle θ of the repulsive force and the driving force satisfy the condition $\theta \in (\pi - \zeta, \pi + \zeta)$ when the distance between the agent and the obstacles is in a specific range, where ζ is the angle threshold of the repulsive force and the driving force, and the agent stops or moves in the opposite direction, then we can judge that the agent is falling into a local minima trap.*

The following is the equation of the normal force:

$$|F_c| = \begin{cases} k_c(1 - \dfrac{\|d_{uo}\|}{\rho_s}), & \rho_s + \rho_o < \|d_{uo}\| \leq \rho_s \\ 0, & \|d_{uo}\| > \rho_s \end{cases} \tag{9}$$

where $|\cdot|$ represents the absolute value, k_c is the normal force coefficient, $\|d_{uo}\|$ is the Euclidean distance between agent and obstacle, ρ_o, ρ_w, ρ_s are positive constants. The magnitude of the normal force increases as the agent approaches the obstacle to prevent falling into local minima. When the angle between the repulsive force and the driving force is not in the angle threshold, it is judged to escape from the local minima.

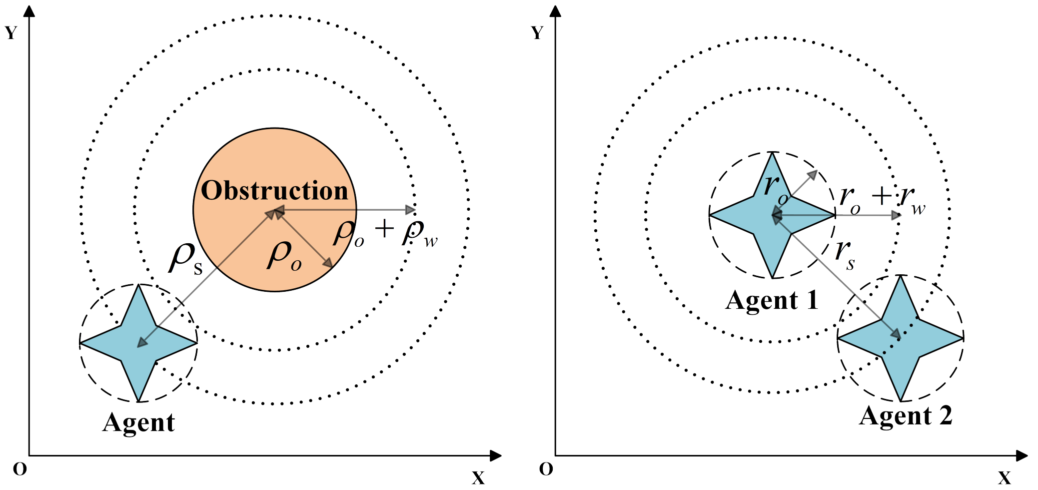

(a) Distances of obstacle avoidance

(b) Distances of collision avoidance

Fig. 2: Different distances of obstacle avoidance and collision avoidance

Remark 2. *It should be noted that the leader, as the agent guiding the follower tracking trajectory, must introduce the normal force, while the follower introduces an external disturbance in the dynamics equation, which does not fall into local minima. Also, for the leader, the direction of the normal force is the vertical direction of the leader's direction of motion.*

In addition, in the actual situation, each agent and each obstacle are entities and are not a point. So, danger, alert, and safety distances should be proposed, as shown in Figure 2(a) and 2(b). Both agents and obstacles have various distances mentioned above, so in this paper, based on the improved APF method for four different cases of obstacle avoidance and collision avoidance, namely, the problem of obstacle avoidance includes the obstacle avoidance of leader and follower, and the problem of collision avoidance includes the collision avoidance between the leader and each follower, and between followers.

Combined with the schematic, the potential field function for obstacle avoidance is as follows [33]:

$$\phi_{oa}(\|d_{oa}\|) = \begin{cases} \Theta_1, & \|d_{oa}\| \in (0, \rho_o + \rho_w) \\ \Theta_2, & \|d_{oa}\| \in (\rho_o + \rho_w, \rho_s) \\ 0, & \|d_{oa}\| \in (\rho_s, +\infty) \end{cases} \tag{10}$$

where $\|d_{oa}\|$ represents the Euclidean distance between obstacle and agents, the first interval $(0, \rho_o + \rho_w)$ represents the danger distance, and the second interval $(\rho_o + \rho_w, \rho_s)$ represents the alarm distance, and the third interval $(\rho_s, +\infty)$ represents the safety distance. Θ_1 is a positive constant, and Θ_2 is as follows:

$$\Theta_2 = \exp \frac{\rho_s - \|d_{oa}\|}{\|d_{oa}\| - \rho_o - \rho_w} - 1 \tag{11}$$

Finally, the non-negative improved potential field functions U_{oa} and repulsive functions F_{oa} are as follows:

$$U_{oa} = \int_{\rho_s}^{\|d_{oa}\|} \phi_{oa}(\|d_{oa}\|) d(\|d_{oa}\|) \tag{12}$$

$$F_{oa} = -\omega_{oa} \nabla U_{oa} = \omega_{oa} \phi_{oa}(\|d_{oa}\|) \frac{d_{oa}}{\|d_{oa}\|} \tag{13}$$

where F_{oa} are the obstacle avoidance forces of leader and follower, respectively, ω_{oa} is a positive gain parameter. $d_{oa} = p_{obstacle} - p_{agent}$ is the relative distance between agent and obstacle.

Likewise, the formula for collision avoidance is as follows:

$$\phi_{ca}(d_{ca}) = \begin{cases} \sigma_1, & \|d_{ca}\| \in (0, r_o + r_w) \\ \sigma_2, & \|d_{ca}\| \in (r_o + r_w, r_s) \\ 0, & \|d_{ca}\| \in (r_s, +\infty) \end{cases} \tag{14}$$

where $\|d_{ca}\|$ represents the Euclidean distance between agents, and the first interval $(0, r_o + r_w)$ represents the danger distance, the second interval $(r_o + r_w, r_s)$ represents the alarm distance. The third interval $(r_s, +\infty)$ represents the safety distance, σ_1 is a positive constant and σ_2 is as follows:

$$\sigma_2 = K \tan \frac{\pi}{2} \left(\frac{\|d_{ca}\| - r_o - r_w}{r_s - r_o - r_w} - 1 \right) \tag{15}$$

where K is a positive constant.

The non-negative improved potential field functions U_{ca} and repulsive functions F_{ca} are as follows:

$$U_{ca} = \int_{r_s}^{\|d_{ca}\|} \phi_{ca}(\|d_{ca}\|) d(\|d_{ca}\|) \tag{16}$$

$$F_{ca} = -\omega_{ca} \sum_{j \in N_i^c} \nabla U_{ca} = \omega_{ca} \sum_{j \in N_i^c} \phi_{ca}(\|d_{ca}\|) \frac{d_{ca}}{\|d_{ca}\|} \tag{17}$$

where F_{ca} are the collision avoidance forces of leader and follower, including collision avoidance force between leader and follower or followers, N_i^c denotes the set of collision avoidance neighbors of the object.

The following lemma is introduced to better complete the proof of the latter theorem:

Lemma 1 ([38]). *The directed graph G is strongly connected if its Laplacian matrix is irreducible.*

Lemma 2 ([5]). *$S(t) > 0$ is a continuous function for any time, and the initial state of $S(0)$ is bounded. If the inequality holds $\dot{S}(t) > qS(t)$ for $t - t_0 \geq 0$ and $q > 0$, then we have the following inequality:*

$$S(t) > e^{q(t-t_0)} S(t_0)$$

III. Controller design and stability analysis

This section includes the design of the formation controller and the design of the controller for collision avoidance and obstacle avoidance, where both designs are also mathematically proven to meet the system requirements, respectively.

A. Formation controller

In complex MAS, there exist many tracking trajectory problems, and graph theory is used to connect these problems in series to accomplish the control objectives. Therefore, in the complex MAS, the formation position and velocity tracking errors $\epsilon_i^p, \epsilon_i^v$and the formation controller input u_i^f of the system are as follows [34]:

$$\begin{aligned}\epsilon_i^p &= \sum_{j\in N_i} a_{ij}(e_i^p - e_j^p) + b_i(e_i^p)\\ \epsilon_i^v &= \sum_{j\in N_i} a_{ij}(e_i^v - e_j^v) + b_i(e_i^v)\end{aligned} \tag{18}$$

$$u_i^f = -\hat{W}_i^\top H_i(z_i) - k_i(\epsilon_i^p + \epsilon_i^v) \tag{19}$$

where $\epsilon_i^p = [\epsilon_{i1}^p, \epsilon_{i2}^p, \cdots, \epsilon_{im}^p]^\top \in \mathbb{R}^m, \epsilon_i^v = [\epsilon_{i1}^v, \epsilon_{i2}^v, \cdots, \epsilon_{im}^v]^\top \in \mathbb{R}^m$, k_i are positive constants, $\hat{W}$ is given in the following form:

$$\dot{\hat{W}}_i(t) = \Gamma(\epsilon_i^p + \epsilon_i^v)H_i(z_i) - \sigma_i \hat{W}_i(t) \tag{20}$$

where Γ and σ_i are positive constants.

B. Obstacle avoidance and collision avoidance controller

According to the above improved APF method, six kinds of control signals are added respectively for formation control u_i^f, and local minima control u_i^{lm}, leader and obstacle avoidance control u_i^{lo}, follower and obstacle avoidance control u_i^{fo}, collision avoidance control u_i^{lf} between follower and leader, collision avoidance control u_i^{ff} between follower, and their controller formulas are as follows:

$$\begin{aligned}u_l &= u_i^{lo} + u_i^{lf} + u_i^{lm}\\ u_i &= \frac{1}{g_i(\cdot)}(u_i^f + u_i^{fo} + u_i^{lf} + u_i^{ff})\end{aligned} \tag{21}$$

where $u_i^{lo}, u_i^{fo} = F_{oa}, u_i^{lf}, u_i^{ff} = F_{ca}, u_i^{lm} = |F_c|$.

Theorem 1. *Consider the MAS with time delay and external disturbance under the formation controller* (19) *and obstacle avoidance controller and collision avoidance controller* (21)*, and choose the correct parameters. The MAS will complete the formation control and obstacle and collision avoidance at the same time.*

Proof: The purpose of obstacle avoidance and collision avoidance is to make the distance between agents or the distance between agents and obstacles will not fall below the threshold, so according to this analysis, this proof will revolve around the relative distance between agents d_{ca} and the relative distance between agents and obstacles d_{oa}.

Define the energy function $S_1(t), S_2(t)$ as follows:

$$S_1(t) = \tfrac{1}{2}d_{ca}^\top(t)d_{ca}(t) + \tfrac{1}{2}v_i^\top(t)vi(t) \tag{22}$$

$$S_2(t) = \tfrac{1}{2}d_{oa}^\top(t)d_{oa}(t) + \tfrac{1}{2}v_l^\top(t)v_l(t) \tag{23}$$

The time derivative of (22):

$$\begin{aligned}\dot{S}_1(t) =& d_{ca}^\top(t)\dot{d_{ca}}(t) + v_i^\top(t)\dot{v_i}(t)\\ =& d_{ca}^\top(t)(\dot{p_i}(t) - \dot{p_j}(t)) + v_i^\top(t)(f_i(\cdot)\\ &+ \delta(t) + g_i(\cdot)u_i(t))\\ =& d_{ca}^\top(t)(v_i(t) - v_j(t)) - v_i^\top \tilde{W_i}^\top(t)H_i(z_i)\\ &- k_i v_i^\top(t)(\epsilon_i^p(t) + \epsilon_i^v(t))\\ &+ v_i^\top(t)f_l(\cdot) + \omega_{ca}v_i^\top(t)\nabla\phi_{ca}(\|d_{ca}\|)\end{aligned} \tag{24}$$

$$\begin{aligned}\dot{S}_2(t) &= d_{oa}^\top(t)\dot{d_{oa}}(t) + v_l^\top(t)\dot{v_l}(t)\\ &= d_{oa}^\top(t)\dot{p_l}(t) + v_l^\top(t)(f_l(\cdot) + u_l)\\ &= d_{oa}^\top(t)v_l(t) + v_l^\top(t)f_l(\cdot) + v_l^\top\omega_{oa}\nabla\phi_{oa}(\|d_{oa}\|)\end{aligned} \tag{25}$$

According to assumptions1, 2, and 3, we know that $f_l, \epsilon_i^p, \epsilon_i^v, v_i(t), v_l(t), \tilde{W}_i(t)H_i(z_i)$ are bounded and the repulsive function $\nabla\phi(\|d_{ca}\|)$ tend to infinity under the condition that the parameters are designed to be large enough. In summary, there are the following inequalities

$$\begin{aligned}&v_i^\top(t)\nabla\phi_{ca}(\|d_{ca}\|) > \frac{1}{2}d_{ca}^\top d_{ca}(t) + \frac{1}{2}v_i^\top(t)v_i(t)\\ &- \frac{1}{\omega_{ca}}d_{ca}^\top(t)(v_i(t) - v_j(t)) + \frac{1}{\omega_{ca}}v_i^\top(t)\tilde{W_i}^\top(t)H_i(z_i)\\ &+ \frac{k_i}{\omega_{ca}}v_i^\top(t)(\epsilon_i^p(t) + \epsilon_i^v(t)) - \frac{1}{\omega_{ca}}v_i^\top(t)f_l(\cdot)\end{aligned} \tag{26}$$

$$\begin{aligned}v_l^\top(t)\nabla\phi_{oa}(\|d_{oa}\|) >& \frac{1}{2}d_{oa}^\top(t)d_{oa}(t) + \frac{1}{2}v_l^\top(t)v_l(t)\\ &- \frac{1}{\omega_{oa}}v_l^\top(t)f_l(\cdot) - \frac{1}{\omega_{oa}}d_{oa}^\top(t)v_l(t)\end{aligned} \tag{27}$$

Substituting the inequality 26 into 24 and 25, respectively:

$$\dot{S}_1(t) > \omega_{ca}S_1(t) \tag{28}$$

$$\dot{S}_2(t) > \omega_{oa}S_2(t) \tag{29}$$

According to 2, the inequality can be obtained

$$d_{ca}^\top(t)d_{ca}(t) > 2e^{\omega_{ca}(t-t_0)}S_1(t) - v_i^\top(t)v_i(t) \tag{30}$$

$$d_{oa}^\top(t)d_{oa}(t) > 2e^{\omega_{oa}(t-t_0)}S_2(t) - v_l^\top(t)v_l(t) \tag{31}$$

Because $v_l(t), v_i(t)$ is continuous and bounded, combined with inequalities (30, 31), we can design the appropriate ω_{ca} and ω_{oa} so that $d_{ca}^2 > (r_o + r_w)^2, d_{oa}^2 > (\rho_o + \rho_w)^2$ is satisfied, which collision avoidance and obstacle avoidance can be guaranteed, the proofs of the other two types avoidance are in the same way. ■

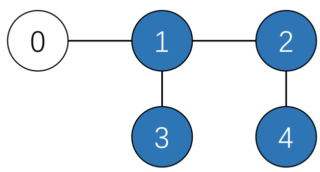

Fig. 3: Communication topology graph

IV. Simulation example

Comparative experiments in the form of simulation will be conducted to verify the robustness of the improved APF algorithm.

First, the topology diagram 3 of leader and follower is given, its B-matrix is $diag[1,0,0,0]$ and its Laplacian matrix is as follows:

$$L=\begin{bmatrix} 2 & -1 & -1 & 0 \\ -1 & 2 & 0 & -1 \\ -1 & 0 & 1 & 0 \\ 0 & -1 & 0 & 1 \end{bmatrix}$$

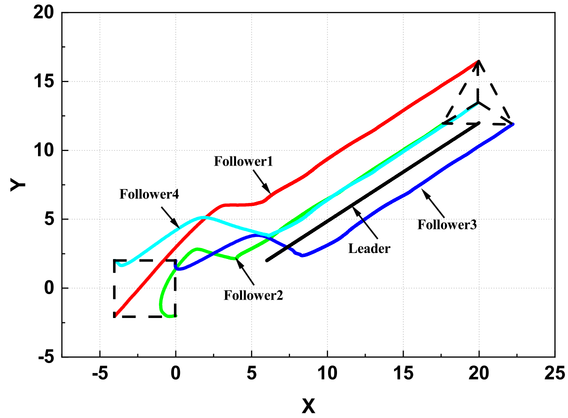

Fig. 4: Trajectory diagram of formation control

Since the simulated system is a MAS based on two-dimensional planar motion, dimension $m=2$, and the number of agents $n=4$, the dynamic equation for the follower agent is as follows:

$$\begin{aligned} \dot{p}_i =& v_i \\ \dot{v}_i =& \begin{bmatrix} \alpha_{i1}\cos^2 p_{i1}v_{i2} \\ \alpha_{i2}\sin^2 p_{i2}v_{i2} \end{bmatrix} + \begin{bmatrix} \sin(t)\cos(t) \\ \sin(t)\cos(t) \end{bmatrix} \\ &+ \begin{bmatrix} 1+\beta_{i1}\cos^2 p_{i1}p_{i2} & 0 \\ 0 & 2+\beta_{i2}\sin^2 v_{i1}v_{i2} \end{bmatrix} u_i \end{aligned}$$

where α,β is given as table I, $\begin{bmatrix} \sin(t)\cos(t) \\ \sin(t)\cos(t) \end{bmatrix}$ is the external disturbance vector, the time delay $\tau=40ms$.

TABLE I: Value of α and β

i	1	2	3	4
α_{i1}	0.3	-0.6	0.5	-0.3
α_{i2}	0.4	0.2	-0.8	-0.9
β_{i1}	0. 3	0.7	0.6	1.3
β_{i2}	0.5	-0.2	-0.8	-1.0

The dynamic equation of the leader agent is designed as follows:

$$\begin{aligned} \dot{p}_l &= v_l \\ \dot{v}_l &= \begin{bmatrix} 0.07 \\ 0.05 \end{bmatrix} + u_l \end{aligned}$$

The initial position of the two agents and the formation position is given as $p_1=[-4,-2]^\top$, $p_2=[0,-2]^\top$, $p_3=[0,2]^\top$, $p_4=[-4,2]^\top$, $p_l=[6,2]^\top$, $\Xi_1=[0,3\chi]^\top$, $\Xi_2=[-\sqrt{3}\chi,0]^\top$,$\Xi_3=[\sqrt{3}\chi,0]^\top$, $\Xi_4=[0,\chi]^\top$, $\chi=\frac{2}{3}$.

The parameters of RBFNN are as follows: the kernel function is chosen as a Gaussian function, the width of the function $K_N=2$, the number of nodes $j=36$, and the range of the composition of numerous nodes is $[-3,3]\times[-3,3]$, for the formula of the update of the neural network weights, $\Gamma=20$, $\sigma_i=0.0001$.

For the control of collision avoidance and obstacle avoidance, the warning distance $r_o=0.2, r_w=0.2$ and the safety distance $r_s=2$ for obstacles, and the warning distance $p_o=0.5, p_w=0.5$ and the safety distance $p_s=2.5$ between agents. The repulsion coefficients of the four repulsion functions are as follows: $\omega_{ca}=1, \omega_{oa}=0.5, K=0.1$. In addition, $k_i=5$, the normal force coefficient $k_c=20$, the threshold of the angle between drive and repulsion $\zeta=30$.

In the absence of environmental obstacles, the overall formation, as illustrated in Figure 4, transforms over time, transitioning from its initial rectangular shape to that of a triangle. Moreover, Lyapunov-based Radial Basis Function (RBF) neural network control enables the accurate adaptation of the uncertain nonlinear dynamical equation, as depicted in Figure 5.

For the consensus of the MAS, we give Figure 6, from which it can be seen that the position and velocity have

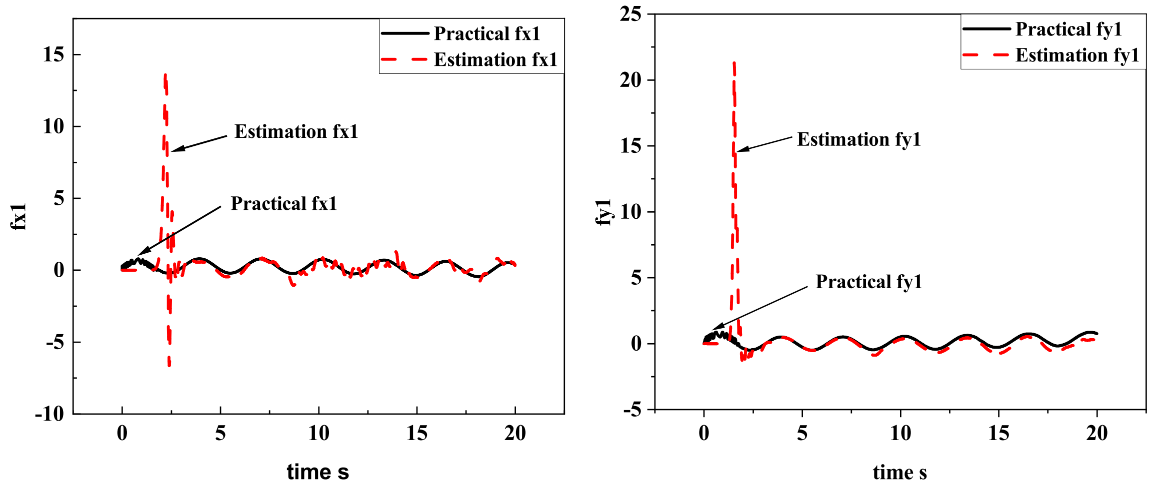

(a) $f_{11}(\cdot)$ (b) $f_{12}(\cdot)$

Fig. 5: Approximation of neural network control

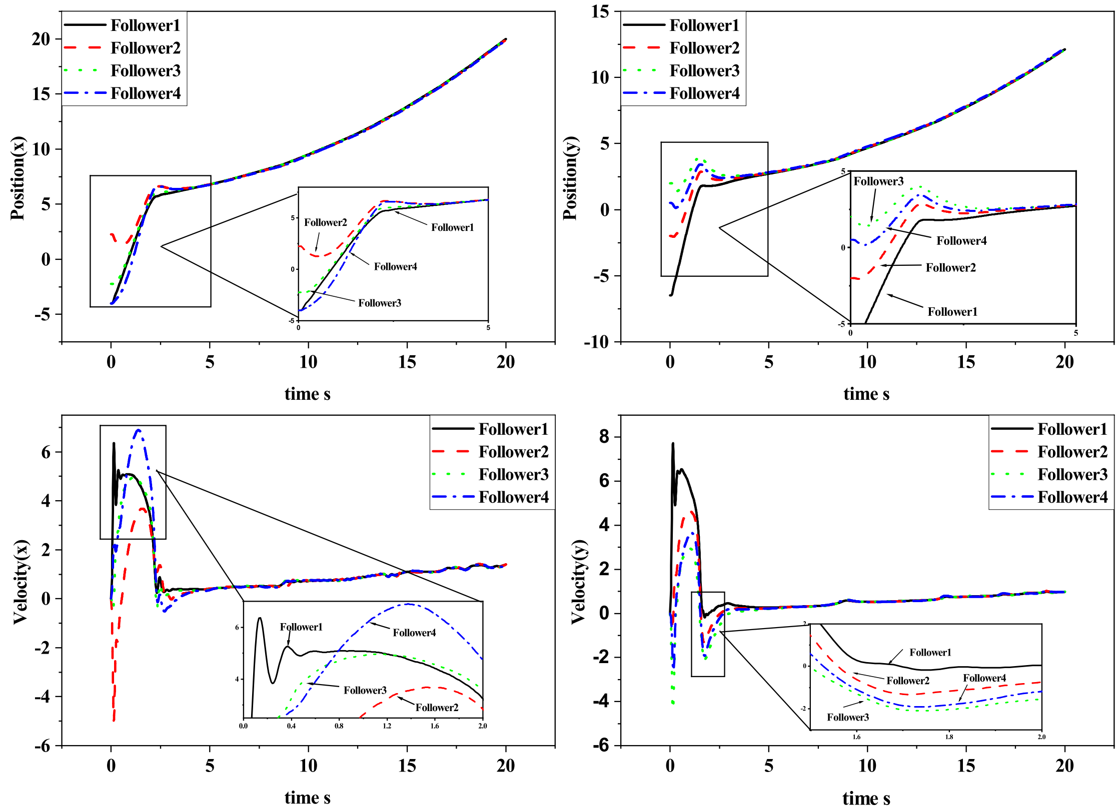

Fig. 6: Consensus of positions, velocity

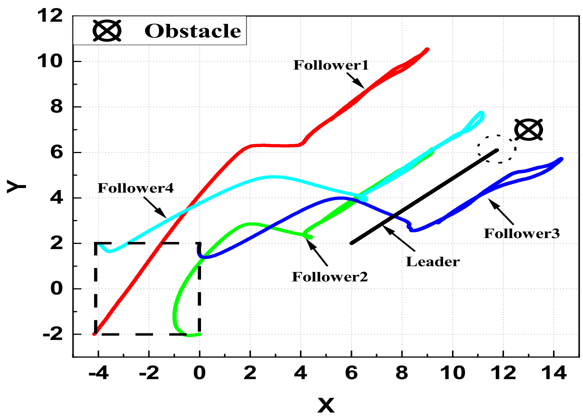

(a) Traditional APF for one obstacle

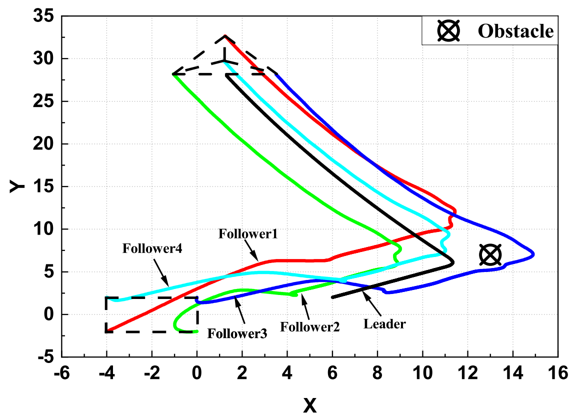

(b) Improved APF for one obstacle

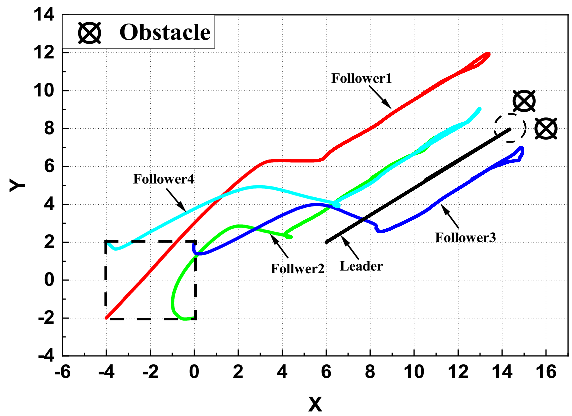

(c) Traditional APF for obstacles

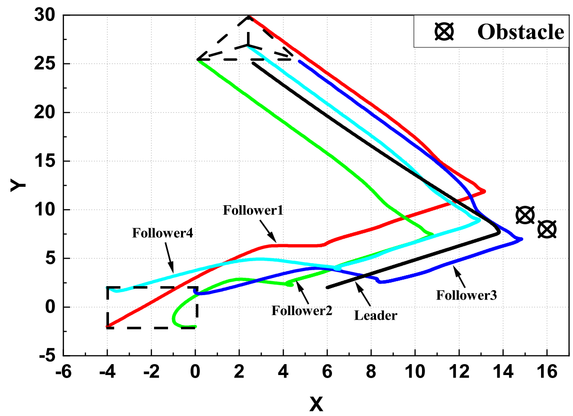

(d) Improved APF for obstacles

Fig. 7: Comparison of traditional APF and improved APF

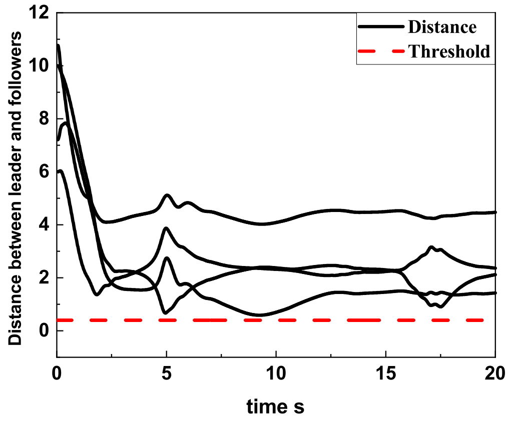

(a) Distance between leader and followers

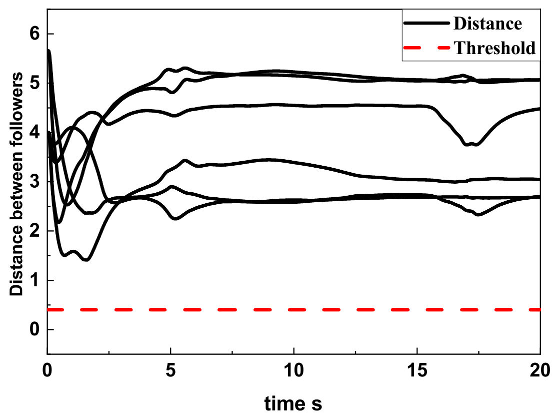

(b) Distance between followers

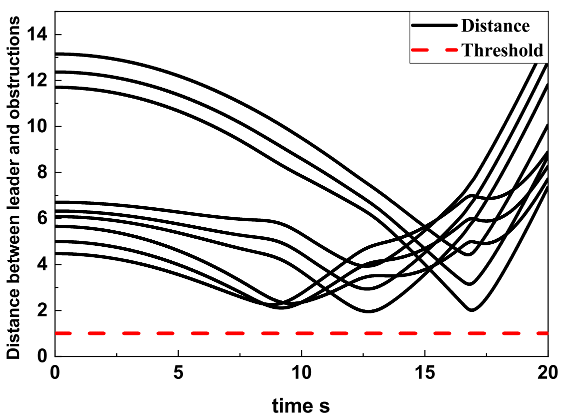

(c) Distance between leader and obstacles

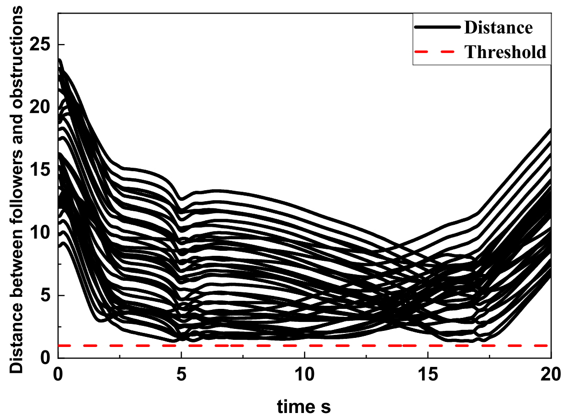

(d) Distance between followers and obstacles

Fig. 8: The distances of four cases

achieved the consensus.

In Figure 7(a), the coordinate of the obstacle is $[13, 7]^\top$, and what can be seen is that the leader agent traps in the local minima similar to Figure 1(a) when using the traditional APF method. However, when we use the improved APF method, as shown in Figure 7(b), the leader agent bypasses the obstacle and keeps moving until the time runs out.

In another case, when there is more than one obstacle, the agent will also fall into local minima, so let the coordinates of the obstacle be $[15, 9.45]^\top, [16, 8]^\top$. In Figure 7(c), it can be seen that the agent is similar to 1(b) when using the traditional APF method. The agent is caught in the local minima when using the improved APF method, and the leader agent will escape from the local minima trap based on the traction of the normal force.

The comparative tests show that the improved APF method is effective compared to the traditional APF method when used in MAS.

To show the superiority of the algorithm's collision avoidance and obstacle avoidance performance, we will give a harsh environment that includes multiple obstacles and changes of initial conditions, and the results can confirm the robustness of the algorithm and the coordinates of the obstacles in the simulation are as follows: $[8, 6]^\top, [9, 6]^\top, [10, 6]^\top, [12, -1]^\top, [12, 0]^\top, [12, 1]^\top, [17, 6]^\top$ $[18, 5]^\top, [19, 4]^\top$. The distances in the four cases are shown in Figure 8, the obstacle avoidance and collision avoidance experiments under four cases are indicated respectively, and the horizontal line in the figure represents the minimum distance of the upcoming collision, i.e., $\rho_o + \rho_w$ and $r_o + r_w$, if it is lower than this value, a collision will occur, so it can be seen that the improved algorithm can realize the collision avoidance and obstacle avoidance requirements under the real sense, and to see the effect of formation obstacle avoidance and collision avoidance more intuitively, the trajectory diagram as shown in Figure 9 is given.

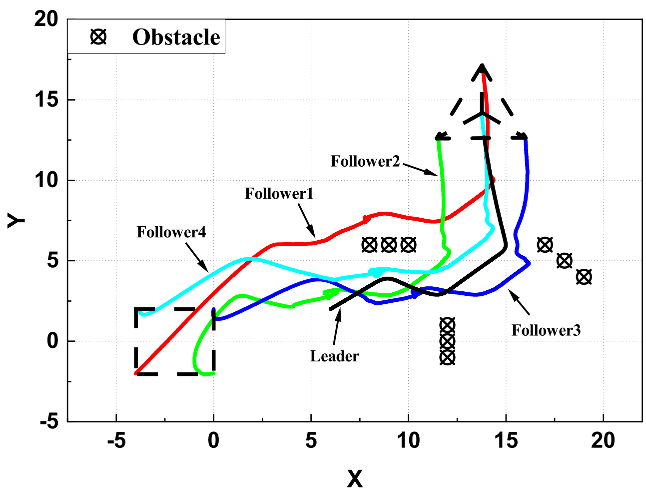

Fig. 9: Formation trajectory diagram of multiple obstacles

V. Conclusions

In this paper, the formation control with external disturbance and time delay for second-order nonlinear MAS were completed by improved APF method and RBFNN adaptive control under the leader-follower framework. External disturbances and time delay conditions often encountered in realistic environments are incorporated into the MAS. Adaptive approximating of unknown complex nonlinear functions in systems using RBFNN. Based on the improved APF method, the problem of trapping in the local minima, which still needs to be solved in most of the papers about MAS formation control, is solved, and four situations of collision avoidance and obstacle avoidance control are also added. At the same time, we give the mathematical proof which can verify the idea above. At last, The simulations were given to confirm the superiority and generality of the algorithm and control design.

Our future work will focus on the problem of high-order MAS formation control and the problem of obstacle avoidance based on dynamic obstacles.

References

[1] Y.-Y. Qian, L. Liu, and G. Feng, "Output consensus of heterogeneous linear multi-agent systems with adaptive event-triggered control," *IEEE Transactions on Automatic Control*, vol. 64, no. 6, pp. 2606–2613, 2019.

[2] Q. Ma and S. Xu, "Consensus switching of second-order multiagent systems with time delay," *IEEE Transactions on Cybernetics*, vol. 52, no. 5, pp. 3349–3353, 2022.

[3] M. Chen and X. Wang, "Flocking dynamics for multi-agent system with measurement delay," *Mathematics and Computers in Simulation*, vol. 171, pp. 187–200, 2020.

[4] T. Li, R. Zhao, C. L. P. Chen, L. Fang, and C. Liu, "Finite-time formation control of under-actuated ships using nonlinear sliding mode control," *IEEE Transactions on Cybernetics*, vol. 48, no. 11, pp. 3243–3253, 2018.

[5] G. Wen, C. Chen, H. Dou, H. Yang, and C. Liu, "Formation control with obstacle avoidance of second-order multi-agent systems under directed communication topology," *Science China Information Sciences*, no. 9, p. 14, 2019.

[6] Y. Hong, J. Hu, and L. Gao, "Tracking control for multi-agent consensus with an active leader and variable topology," *Automatica*, vol. 42, no. 7, pp. 1177–1182, 2006.

[7] W. Guo, J. Lü, S. Chen, and X. Yu, "Second-order tracking control for leader–follower multi-agent flocking in directed graphs with switching topology," *Systems and Control Letters*, vol. 60, no. 12, pp. 1051–1058, 2011.

[8] M. Egerstedt, X. Hu, and A. Stotsky, "Control of mobile platforms using a virtual vehicle approach," *IEEE Transactions on Automatic Control*, vol. 46, no. 11, pp. 1777–1782, 2001.

[9] R. W. Beard, J. Lawton, and F. Y. Hadaegh, "A coordination architecture for spacecraft formation control," *IEEE Transactions on Control Systems Technology*, vol. 9, no. 6, pp. 777–790, 2001.

[10] J. R. Lawton and R. W. Beard, "Synchronized multiple spacecraft rotations," *Automatica*, vol. 38, no. 8, pp. 1359–1364, 2002.

[11] J. Hu, Y. Wu, T. Li, and B. K. Ghosh, "Consensus control of general linear multiagent systems with antagonistic interactions and communication noises," *IEEE Transactions on Automatic Control*, vol. 64, no. 5, pp. 2122–2127, 2019.

[12] W. Wang, C. Wen, and J. Huang, "Distributed adaptive asymptotically consensus tracking control of nonlinear multi-agent systems with unknown parameters and uncertain disturbances," *Automatica*, vol. 77, pp. 133–142, 2017.

[13] Y.-P. Tian and Y. Zhang, "High-order consensus of heterogeneous multi-agent systems with unknown communication delays," *Automatica*, vol. 48, no. 6, pp. 1205–1212, 2012.

[14] H. Du, G. Wen, D. Wu, Y. Cheng, and J. Lü, "Distributed fixed-time consensus for nonlinear heterogeneous multi-agent systems," *Automatica*, vol. 113, p. 108797, 2020.

[15] Z. Li, T. Li, G. Feng, R. Zhao, and Q. Shan, "Neural network-based adaptive control for pure-feedback stochastic nonlinear systems with time-varying delays and dead-zone input," *IEEE Transactions on Systems, Man, and Cybernetics: Systems*, vol. 50, no. 12, pp. 5317–5329, 2020.

[16] Y. Wang, Y. Gu, X. Xie, and H. Zhang, "Delay-dependent distributed event-triggered tracking control for multi-agent systems with input time delay," *Neurocomputing*, vol. 333, pp. 200–210, 2019.

[17] T. Xiong and Z. Gu, "Observer-based adaptive fixed-time formation control for multi-agent systems with unknown uncertainties," *Neurocomputing*, vol. 423, pp. 506–517, 2021.

[18] F. Mehdifar, C. P. Bechlioulis, F. Hashemzadeh, and M. Baradarannia, "Prescribed performance distance-based formation control of multi-agent systems," *Automatica*, vol. 119, p. 109086, 2020.

[19] Y. Guo, J. Zhou, G. Li, and J. Zhang, "Robust formation tracking and collision avoidance for uncertain nonlinear multi-agent systems subjected to heterogeneous communication delays," *Neurocomputing*, vol. 395, pp. 107–116, 2020.

[20] C. L. P. Chen, G.-X. Wen, Y.-J. Liu, and Z. Liu, "Observer-based adaptive backstepping consensus tracking control for high-order nonlinear semi-strict-feedback multiagent systems," *IEEE Transactions on Cybernetics*, vol. 46, no. 7, pp. 1591–1601, 2016.

[21] G. Wen, C. L. P. Chen, Y.-J. Liu, and Z. Liu, "Neural network-based adaptive leader-following consensus control for a class of nonlinear multiagent state-delay systems," *IEEE Transactions on Cybernetics*, vol. 47, no. 8, pp. 2151–2160, 2017.

[22] Y. Fei, P. Shi, and C.-C. Lim, "Neural network adaptive dynamic sliding mode formation control of multi-agent systems," *International Journal of Systems Science*, vol. 51, no. 11, pp. 2025–2040, 2020.

[23] J. Wang and M. Xin, "Multi-agent consensus algorithm with obstacle avoidance via optimal control approach," in *Proceedings of the 2011 American Control Conference*, pp. 2783–2788, 2011.

[24] A. J. Häusler, A. Saccon, A. P. Aguiar, J. Hauser, and A. M. Pascoal, "Energy-optimal motion planning for multiple robotic vehicles with collision avoidance," *IEEE Transactions on Control Systems Technology*, vol. 24, no. 3, pp. 867–883, 2016.

[25] H. Xiao, Z. Li, and C. L. Philip Chen, "Formation control of leader–follower mobile robots' systems using model predictive control based on neural-dynamic optimization," *IEEE Transactions on Industrial Electronics*, vol. 63, no. 9, pp. 5752–5762, 2016.

[26] L. Dai, Q. Cao, Y. Xia, and Y. Gao, "Distributed mpc for formation of multi-agent systems with collision avoidance and obstacle avoidance," *Journal of the Franklin Institute*, vol. 354, no. 4, pp. 2068–2085, 2017.

[27] W. Bai, T. Li, and S. Tong, "NN reinforcement learning adaptive control for a class of nonstrict-feedback discrete-time systems," *IEEE Transactions on Cybernetics*, vol. 50, no. 11, pp. 4573–4584, 2020.

[28] A. Mendo, J. Outes-Carnero, Y. Ng-Molina, and J. Ramiro-Moreno, "Multi-agent reinforcement learning with common policy for antenna tilt optimization," in *IAENG International Journal of Computer Science*, vol. 50, pp. 883–889, 2023.

[29] M. I. L. Zeng, G. Chen, and B. Yang, "Multi-agent planning based on causal graphs: From theory to experiment," in *IAENG International Journal of Computer Science*, vol. 49, pp. 55–60, 2022.

[30] Z. Wu, W. Su, and J. Li, "Multi-robot path planning based on improved artificial potential field and b-spline curve optimization," in *2019 Chinese Control Conference (CCC)*, pp. 4691–4696, 2019.

[31] D. Wang, P. Wang, X. Zhang, X. Guo, Y. Shu, and X. Tian, "An obstacle avoidance strategy for the wave glider based on the improved artificial potential field and collision prediction

model," *Ocean Engineering*, vol. 206, p. 107356, 2020.
[32] Q. Shi, T. Li, J. Li, C. P. Chen, Y. Xiao, and Q. Shan, "Adaptive leader-following formation control with collision avoidance for a class of second-order nonlinear multi-agent systems," *Neurocomputing*, vol. 350, pp. 282–290, 2019.
[33] S. Yang, W. Bai, T. Li, Q. Shi, Y. Yang, Y. Wu, and C. L. P. Chen, "Neural-network-based formation control with collision, obstacle avoidance and connectivity maintenance for a class of second-order nonlinear multi-agent systems," *Neurocomputing*, vol. 439, pp. 243–255, 2021.
[34] G. Wen, C. L. P. Chen, and Y.-J. Liu, "Formation control with obstacle avoidance for a class of stochastic multiagent systems," *IEEE Transactions on Industrial Electronics*, vol. 65, no. 7, pp. 5847–5855, 2018.
[35] A. Mondal, L. Behera, S. R. Sahoo, and A. Shukla, "A novel multi-agent formation control law with collision avoidance," *IEEE/CAA Journal of Automatica Sinica*, vol. 4, no. 3, pp. 558–568, 2017.
[36] W. Guo, F. Austin, S. Chen, and W. Sun, "Pinning synchronization of the complex networks with non-delayed and delayed coupling," *Physics Letters A*, vol. 373, no. 17, pp. 1565–1572, 2009.
[37] T.-C. Chen and V. Soo, "Feature selection in learning common sense associations using matrix factorization," *International Journal of Fuzzy Systems*, vol. 19, pp. 1217–1226, 2017.
[38] F. L. Lewis, H. Zhang, K. Hengster-Movric, and A. Das, *Cooperative control of multi-agent systems: optimal and adaptive design approaches*. Springer Science & Business Media, 2013.